Coastal Dynamics 2017
Paper No. 208

Alongshore variability in observed runup under dissipative conditions

Nadia Senechal[1]

Abstract

Alongshore variability in runup dynamics was investigated on a sandy barred beach using data obtained from video images under stationary energetic conditions. Runup was estimated at 8 cross-shore transects situated along a complex 3D morphology. Significant runup height was found to vary by a factor of 4 between the different transects. This increase was essentially driven by the infragravity energy. Data show that environmental parameters as beach slope, bar-shoreline distance and offshore significant wave height do not fully explain this variability. Observations rather suggest that wave transformation (dissipation, harmonic release, refraction, interaction with surf zone circulation) occurring on short distance between the inner bar and the shoreline might be the keys driving parameters. Nonlinear triads and harmonic release are found to be significantly alongshore variable.

Key words: runup, video, infragravity, alongshore variability, wave transformation

1. Introduction

Wave induced runup is defined as the time-varying position of the water's edge on the foreshore of the beach, resulting from a (quasi) steady component above the still water level (the wave setup) and a time-varying fluctuating component (the "swash"). Wave-induced runup is one of the critical parameters used in coastal studies, especially when estimating the probability of extreme water levels and associated possible effects of coastal inundation (e.g. Cohn and Ruggiero, 2016 ; Peregrine and Williams, 2001); and dune and beach erosion (e.g. Palmsten and Splinter, 2016; Ruggiero et al., 2001; Sallenger, 2000).

Predicting wave runup elevations has thus received increasing interest the past decades and yet for a given offshore climate it still remains extremely complicated. Even the most recently developed formulations do not explain the variability encountered in the field (e.g. Stockdon et al., 2014). Earlier studies have rapidly highlighted that swash characteristics (often summarized in term of vertical runup height R) were primarily related to offshore wave characteristic and beach slope (e.g. Holman, 1986; Holman and Sallenger, 1985; Guza and Thornton, 1982). Thus similarly to the surf zone approach, the Iribarren number, defined as:

$$\xi_0 = \frac{\tan\beta}{\left(H_0/L_0\right)^{1/2}} \tag{1}$$

where β is the beach slope, L_0 is the deep water wavelength given by linear theory and H_0 is the offshore significant wave height, has been commonly used to classify the swash. Dissipative swash conditions are generally associated with low values of Iribarren parameters, typically less than 0.3 (Stockdon et al., 2006; Ruggiero et al., 2001; Ruessink et al., 1998, Raubenheimer and Guza, 1996; Raubenheimer et al., 1995; Guza and Thornton, 1982), whereas intermediate and reflective conditions are associated to larger values (Holland and Holman, 1999; Holland, 1995; Holman, 1986; Holman and Sallenger, 1985).

While the role of offshore characteristics is relatively well-defined, the relationship between runup height and other environmental parameters remains elusive. Recent works have already indicated that large- (Ruggiero et al., 2004) and small-scale (Bryan and Coco, 2010) alongshore variations in beach slope give rise to a range of behaviours that complicates prediction of runup height. Guedes et al. (2012) and Senechal et al. (2013) also showed that under both mild and dissipative offshore wave conditions, the

[1]Bordeaux University, UMR EPOC, Pessac, France. nadia.senechal@u-bordeaux.fr

presence of a sandbar and the tidally controlled water-depth over its crest generated important variations (by a factor 2) of significant runup height. The influence of the sandbar configuration on runup has been further investigated by Cohn and Ruggiero (2016) using numerical approach. However Plant and Stockdon (2015) highlighted that there is still a lack of data set to evaluate the benefit of new parameterizations. Our objective is thus to further investigate alongshore variability in runup in presence of a complex 3D bar and under moderate but yet dissipative conditions using an extensive data set collected in the field. Following the results presented by Senechal et al. (2013), additional transects were generated at low tide to allow investigating the impact of the ‘large scale’ morphology and the local parameters.

2. Materials and Methods

2.1. *Field area*

Figure 1. (Left) Field site Truc Vert beach situated on the southern part of the French Atlantic coast. (Right) Aerial view of Truc Vert beach at low tide. Inner bar systems exhibiting a Transverse Bar and Rip configuration are observed on the lower beach, outer subtidal bar horns can be distinguished through the foam of the breaking waves (Right).

Data discussed here were collected during the ECORS field experiment (Senechal et al., 2011a) at Truc Ver t beach situated on the southern part of the French Atlantic coast (Figure 1 left). The sediment consists primarily of medium grained quartz sand whose mean surface grain size is around 0.35 mm but presents variations in relation with the morphology, with coarser sediments (~0.6 mm) observed in the deeper rip channels and finer sediments (~0.3 mm) observed on the shoals between the rips (Gallagher et al., 2011). Complex three-dimensional and highly dynamic morphologies are commonly observed at Truc Vert beach comprising two distinct sandbar systems. The inner bar generally situated in the intertidal domain (Figure 1 right) can experience all the states within the intermediate classification but generally exhibits a Transverse Bar and Rip configuration (see Senechal et al., 2009; Wright and Short, 1984). The outer bar system situated in the subtidal domain exhibits persistent crescentic patterns at a narrow range of wavelengths with a shape varying from symmetric to asymmetric (Castelle et al., 2007). Despite meso- to macrotidal conditions associated with an annual mean spring tidal range of 3.7 m, alongshore tide-driven currents in the nearshore zone are negligible. The wave climate is energetic with an annual mean significant wave height of 1.36 m and mean period around 8 s associated with long distance swells travelling mainly from N-NW directions (Butel et al., 2002).

2.2. *Field data*

Sea state conditions were measured with a directional Mark III Datawell waverider buoy anchored in 55 m depth situated offshore of the field area (Figure 1 left). A synchronous, 5 Hz coherent 7-element alongshore-lagged array of co-located pressure and horizontal digital electromagnetic velocity sensors (hereafter PUV) mounted to pipes jetted along the inner bar was used to evaluate the wave characteristics in the surf zone (Figure 2, bottom black circle). The instruments were located approximately 35 cm from the seabed, cabled to the shore and time-synced to an onshore GPS clock. Throughout the experiment, runup was measured with a video system (see Senechal et al., 2011b for a detailed presentation of the system). To extract runup elevations along individual transects from video, the topography of the beach is needed in addition to the geometry of the cameras. To obtain the beach surface topography, a survey using Real Time Kinematic Differential Global Positioning System (RTK DGPS) was performed at the same time. The vertical resolution of the swash elevation, depending both on lens properties and distance from the cameras, was estimated by mapping the horizontal pixel resolution (typically < 1.0 m) to the elevation along the cross-shore transect. The vertical resolution was less than 0.10 m for all the data analyzed in this work.

As our main interest is in alongshore variability of runup in presence of complex 3D morphologies, the data discussed in this paper will focus on low tide when the lower and complex intertidal domain experiences swash conditions. Data were collected under neap tide conditions to allow for the collection of longer

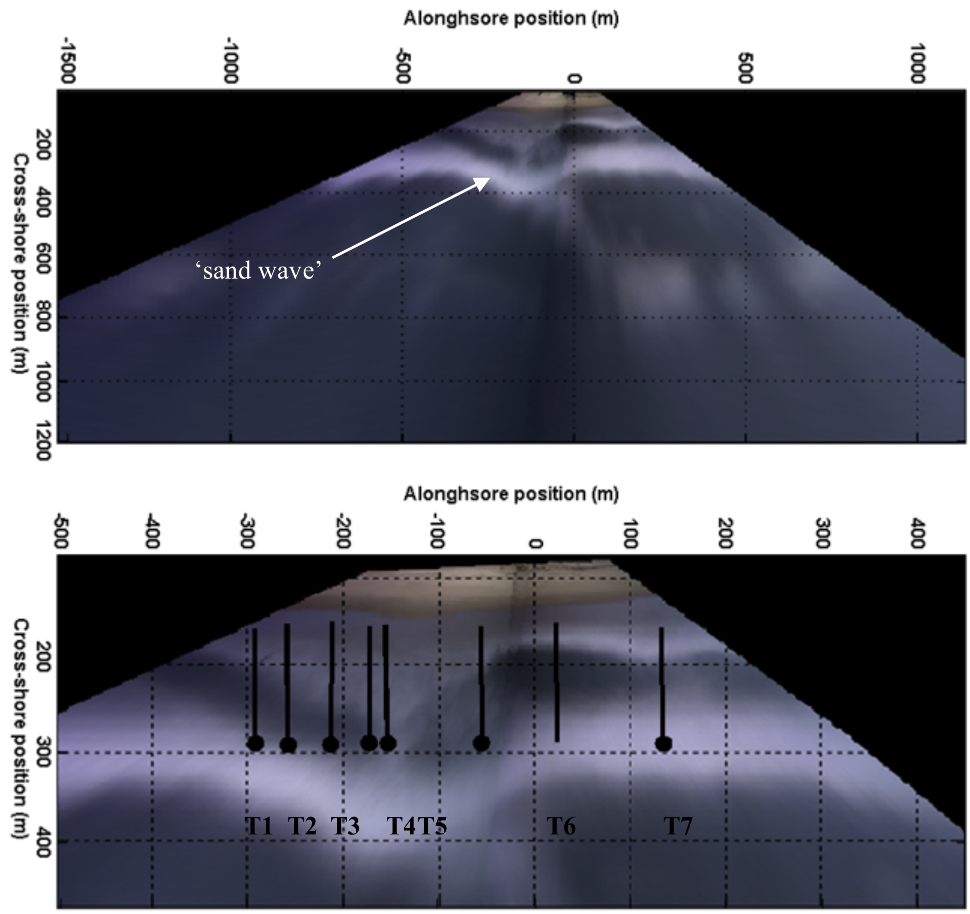

Figure 2. (Top) 10-min averaged rectified image of the field site at low tide highlighting the complex morphology of the inner bar and the lower beach face. (Bottom) Zoom of the previous image with location of the transects (solid lines) and the PUV sensors (black circle).

(stationary) data series. The data discussed below consist of 112 15-min wave runup elevation time series measured along 8 individual cross-shore transects ((Figure 2, denoted as T1, T2, T3…..) situated onshore the PUV sensors deployed on the inner bar despite transect T7 for which no PUV sensor was deployed. This corresponds to 4 consecutive hours centered on low tide for each transect. The generated transects allowed a good coverage of the complex 3D morphology observed in the lower intertidal domain. The sampling frequency of the video system and of the derived runup time series was 2 Hz. The mean water level elevations for the time series considered, according to in-situ pressure measurements, varied by less than 0.4 m.

2.3. *Data processing*

Energy spectra, PSD (f), were computed from detrended, tapered data segments of 1800 points (900 s). The swash and surfzone data were then partitioned to determine the incident band component (0.05 Hz < f < 0.24 Hz) and the infragravity band component (0.004 Hz < f < 0.05 Hz). Swash and surfzone heights, respectively R and *S*, were calculated as:

$$R = 4 * \sqrt{\sum PSD(f)df} \tag{2}$$

Swash and surfzone heights in the incident band, R_{inc}, and in the infragravity band, R_{ig}, were calculated by summing only over frequencies within the specified limits.

Following Guedes et al. (2012), in order to evaluate the possible competing role of the alongshore versus temporal variability in the runup and surf zone parameters, the proportion of the total variance explained by the temporal P_t and spatial P_y component were defined as:

$$\begin{aligned} P_t &= \frac{\left[\langle \chi(t,y) \rangle - \chi_m\right]^2}{\left\langle \left[\chi(t,y) - \chi_m\right]^2 \right\rangle} \\ P_y &= \frac{\left\langle \left[\chi(t,y) - \chi_m\right]^2 \right\rangle}{\left\langle \left[\chi(t,y) - \chi_m\right]^2 \right\rangle} \end{aligned} \tag{3}$$

where χ is a generic runup or surfzone parameter, overbar and angle bracket denote respectively temporal and spatial average and subscript m denotes average over the whole dataset.

Finally, the definition of the foreshore beach slope $\beta_{2\sigma}$ in this study was taken, in agreement with other studies of swash zone hydro- and morphodynamics (e.g. Senechal et al., 2011b; Coco et al., 2004; Ruggiero et al., 2004) to be the linear slope within the region between ± two standard deviations from the mean swash elevation.

3. Results

3.1. *Environmental conditions*

Environmental conditions are provided in figure 3. The selected period (Figure 3, rectangle) corresponds to the neap low tide observed after the very energetic period experienced by the beach on March, 11. During this very energetic storm, mean significant wave heights reached more than 8 m with associated wave period of 16 s. Runup observations were reported to be saturated in the infragravity band (Senechal et al., 2011b) and the beach morphology experienced an up-state transition. In particular, the straightening of the outer bars was observed as well as a Shoreward Propagating Accretionary Wave (SPAW) resulting from the shedding of the horns of the outer bars (Almar et al., 2010). Dramatic morphological changes were also observed in the inner bar and the lower beach face, which both exhibited complex 3D patterns after this event with the presence of a 'sand wave' between transects T1 and T6 (Figure 2 bottom). This probably explains why despite energetic conditions observed during the selected period and characterized by mean significant wave height of 2 m and associated wave peak period of nearly 14 s, no significant wave breaking patterns were observed on the outer bar system even at low tide (Figure 2 Top). The selected period also corresponds to a remarkably stationary period as underlined by Senechal et al. (2013).

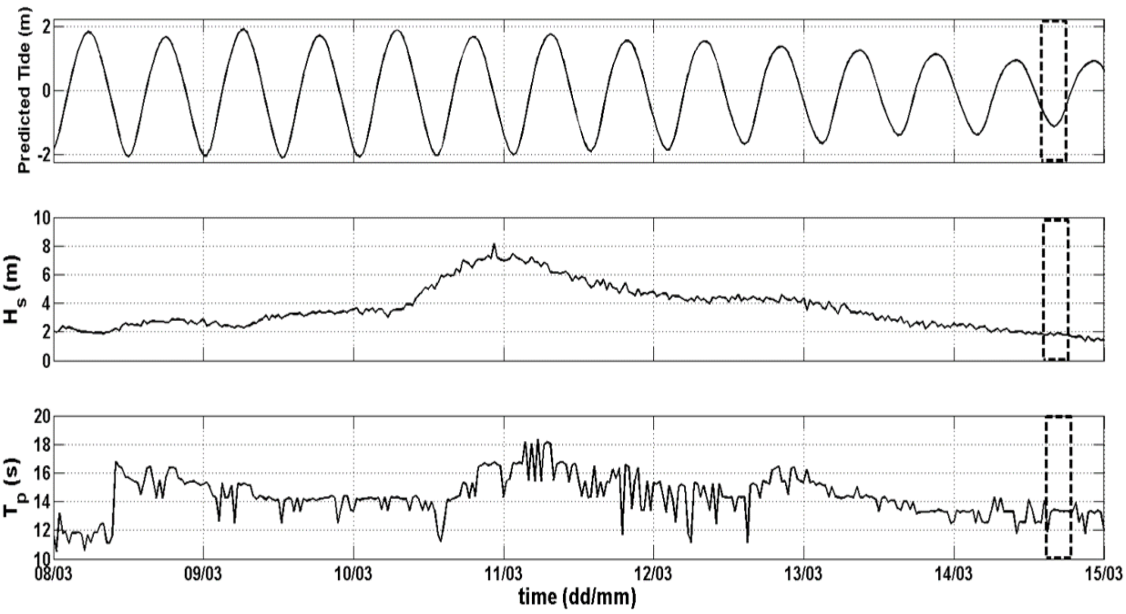

Figure 3. Environmental conditions. (Top) Predicted tide; (Middle) offshore significant wave height (m) and (Bottom) peak period (s) as measured by a wave buoy in 55m water depth offshore of the field area.

Figure 4 illustrates the beach profiles at the different transects. Beach profiles exhibited concave profiles and $\beta_{2\sigma}$ slopes were relatively gentle, typically less than 0.032, consistent with the highly dissipative conditions experienced previously and the selected period coinciding with low-tide. Alongshore range of foreshore beach slope was less than 0.010 accounting for an increase of 43% from the smallest (0.025) to the highest value (0.032) and was essentially due to the presence on one hand of a rip channel close to Transect T 7 and on the other hand of the 'sand wave' at Transects T 1 – T 6 (Figure 2).

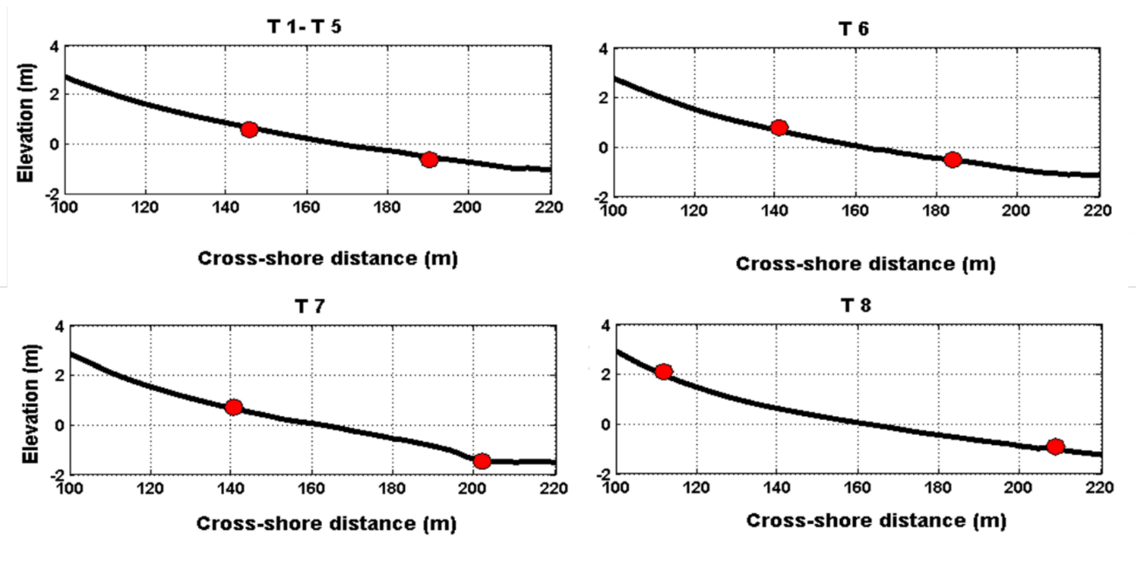

Figure 4. Beach profiles at the different transect locations. Onshore and offshore limits (mean ± 2 standard deviations) of swash excursion for each transect are indicated by red circles.

Alongshore variation in $\beta_{2\sigma}$ slopes was substantially lower than the ones previously reported in the literature focusing on alongshore variability in swash motions (e.g. Guedes et al., 2012; Ruggiero et al., 2004) but allowed filling in the gap between extremely dissipative conditions (e.g. Ruggiero et al., 2004) and more reflective conditions (e.g. Guedes et al., 2012).

Figure 4 also clearly highlights that the horizontal excursion of run-up (red circles) was relatively short for Transects T 1- T 6 (typically less than 40 m) but could extend up to 100 m at Transect T 8.

3.2. *Runup and Surfzone Energy Spectra*

Figure 5 shows the averaged runup spectra and the averaged surfzone elevation spectra calculated over the 4-hour window at the different alongshore positions. Averaged spectra were calculated from averaging all the 15-min time series for each transect, resulting in 30 degrees of freedom with a bandwidth of 0.0011 Hz.

Concerning the runup spectra, both the relative magnitude between the incident and infragravity runup bands and the shape of the spectra featured alongshore variability. For all transects, the average runup spectra reveal a saturated region that decayed approximately as f^{-3} (despite Transect 7 that decayed at approximately $f^{5/2}$), consistent with previous observations (Ruessink et al. 1998; Guza and Thornton, 1982). Ruggiero et al. (2004) under similar offshore conditions but in presence of very gently beach slopes compared to the present study, found a saturated run-up spectra with an f^{4} roll off rather than the f^{-3}. The knickpoint between the saturated and unsaturated part, estimated using the method described by Ruessink et al. (1998) ranged from approximately 0.021 Hz to 0.033 Hz with a mean of 0.025 Hz; that is, the saturated tail extended into the infragravity-frequency band consistent with previous observations (Senechal et al., 2011b ; Ruggiero et al., 2004; Ruessink et al., 1998). One of the most obvious features in the runup spectra are the overall increase of magnitude in infragravity energy from Transect 1 to Transect 8.

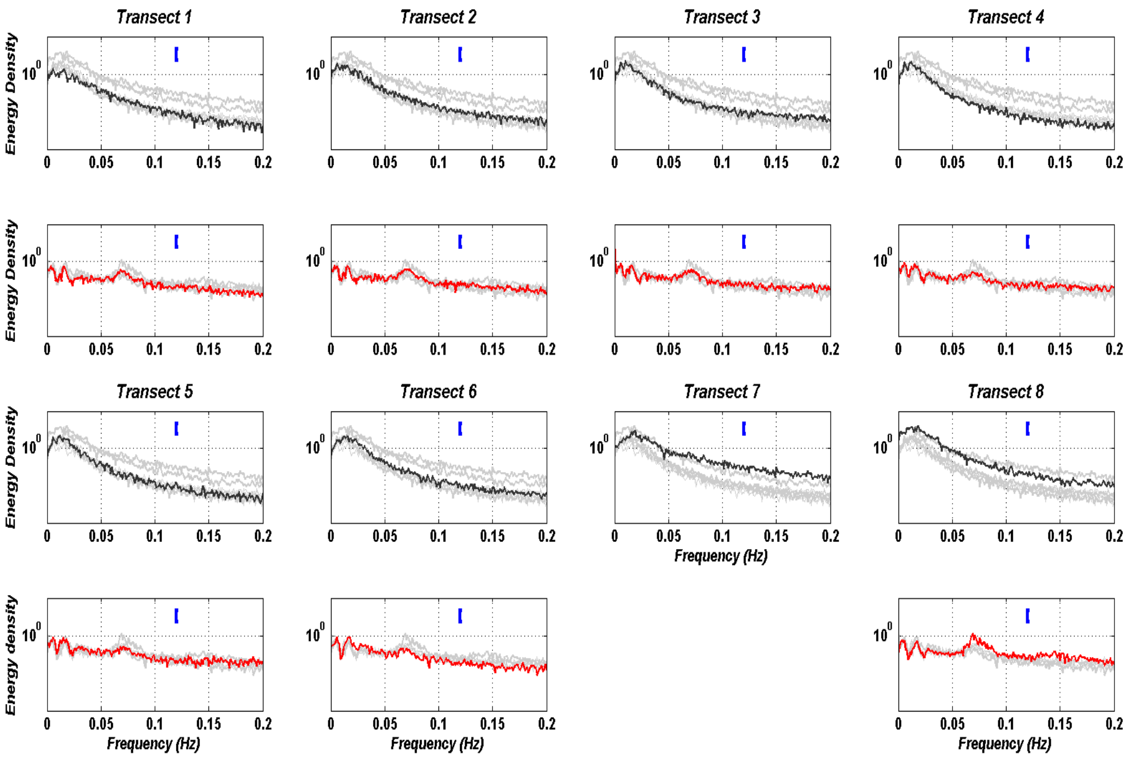

Figure 5. Mean energy density spectra calculated in the swash zone from the runup time series (black lines) and in the surf zone from the elevation time series (red lines) at the different locations. The grey lines represent the swash/surf mean spectra measured at the other locations. The blue vertical line represents the 95% confident interval.

Concerning the surfzone spectra, they also reveal a saturated tail but at high frequencies, typically frequencies greater than $5f_p$ where f_p is the incident peak frequency (not shown on the figure). In contrast with the runup spectra, less alongshore variability is observed both in shape and energy and essentially concerns the energy associated with the incident peak frequency. We observe the presence of energy peaks in the infragravity band, approximately at 0.015 Hz (60 s) for all transects.

3.3. *Runup and Surfzone parameters*

Figure 6 (Left) shows the alongshore series of both swash parameters (blue symbols) and surfzone parameters estimated at the PUV sensors (black symbols). Each value corresponds to the mean value calculated by averaging the values estimated from all the 15-min time series using equation 2. In Figure 6, each value is thus represented by a symbol (the mean) and the associated standard deviation.

Data indicate that swash energy (blue symbols) was dominated by the infragravity energy consistent with observations under dissipative conditions (e.g. Senechal et al., 2011b; Ruggiero et al., 2001). A consistent alongshore trend is observed between transect T 1 and transect T 8 for total swash elevation Rt with values normally lower at transects T 1 – T 4 situated on the ‘sand wave ‘(Figure 1) and then increasing toward transect T 8 (situated onshore the rip channel). The increase in total swash elevation is essentially driven by the increase in the infragravity components even if we observe a clear increase in incident component at transects T 7 and T 8. On the other hand surfzone parameters (black symbols) show a remarkably uniform trend with alongshore ranges in Ht and Hig being less than 0.1m. However we observe that at transect T 8, Hin is significantly higher. No PUV sensor was deployed at transect T 7, explaining the lack of data. Figure 6 (Right) also shows that the observed alongshore variability cannot be only explained by the local beach slope estimated on the beach face (e.g. Ruggiero et al., 2004).

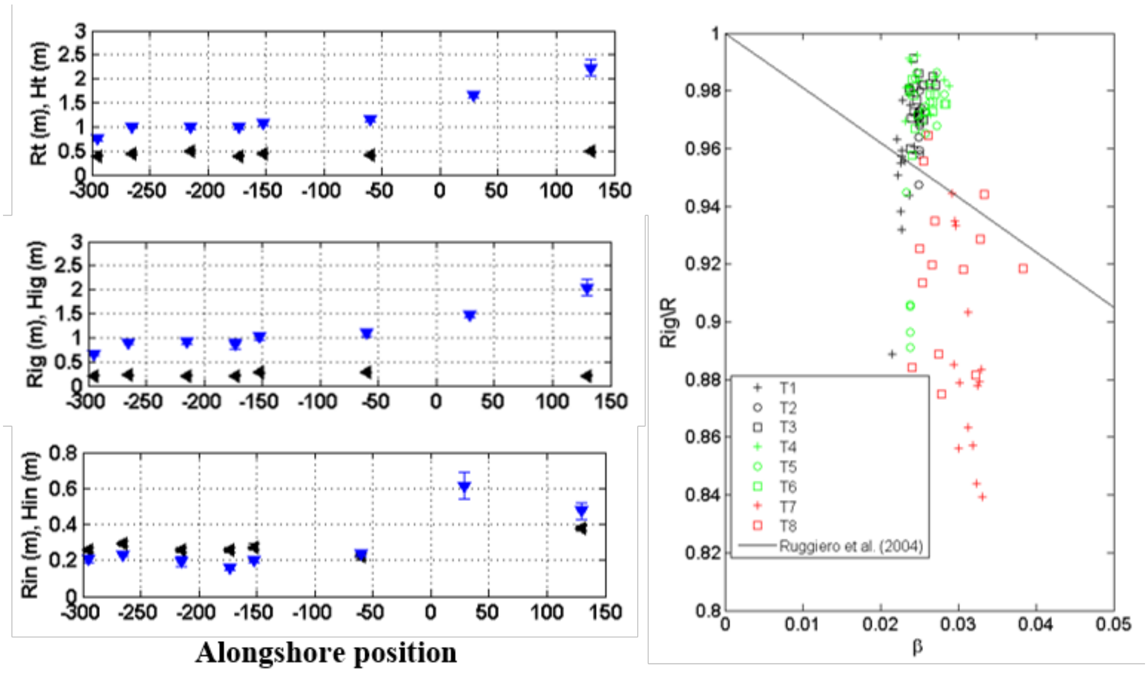

Figure 6. (Left) Alongshore variability of mean parameters. Total, Infragravity and incident components of runup elevations (blue) and at ‘surf zone’ PUV locations (black). (Right) Comparison with the parameterisation proposed by Ruggiero et al. (2004)

According that data were acquired on a 4 hour window centered on low tide (mean sea level variations < 0.4 m) under remarkably stationary offshore conditions, temporal variability was assumed to be weak. Following Guedes et al. (2012), in order to evaluate the possible competing role of the alongshore versus temporal variability in the runup (denoted as R) and surf zone parameters (denoted as H), the proportion of the total variance explained by the temporal P_t and spatial P_y were estimated (equation 3) and are summarized in Table 1. The spatial contributions to the total variance P_y were always greater than the temporal contributions P_t for all runup and surf zone parameters. Concerning the runup parameters, the spatial contribution P_y was an order of magnitude higher than the temporal contribution P_t. Concerning the surfzone parameters, the spatial contribution P_y was a factor 2 to 5 higher than the temporal contribution P_t.

Table 1. Proportion of the total variance in the space-time series χ explained by their temporal P_t and spatial P_y contributions.

χ	**Pt**	**Py**
Rt	0.04	0.87
Rig	0.06	0.83
Rin	0.04	0.82
H	0.29	0.58
Hig	0.14	0.66
Hin	0.28	0.72

The influence of surfzone parameters on the swash parameters was further investigated using regression analysis (the results of linear regression are reported in Table 2). A significant linear regression was observed for all transects between swash elevations in the different frequency component and incident surfzone elevations with correlation coefficients around 0.48 (all significant with p-value < 0.01). Less evident is the lack in correlation between swash elevation in the infragravity component and infragravity energy in the surfzone.

Table 2. Linear regression results. Coefficient correlation r^2 significant at the 99% confidence level are showed in bold.

	Dependent variable	**Independent variables**	**m**	**b**	$\mathbf{r^2}$
All transects	Rt	Ht	4.15	-0.63	**0.21**
		Hig	1.15	0.11	0.00
		Hin	5.87	-0.46	**0.45**
	Rig	Ht	3.87	-0.61	**0.19**
		Hig	0.95	0.50	0.00
		Hin	5.39	-0.43	**0.41**
	Rin	Ht	0.86	-0.13	**0.17**
		Hig	-0.19	0.29	0.00
		Hin	1.39	-0.14	**0.48**

4. Preliminary Discussion

Runup data collected on 8 transects deployed along a complex 3D morphology show a significant increase of runup energy (up to 300%) between transect T 1 and transect T 8, essentially driven by the increase in infragravity energy. Our data also indicate that alongshore variations in swash parameters can neither be explained only by alongshore variations in beach slope as observed under similar dissipative conditions by Ruggiero et al. (2001) nor by variation in the distance from shoreline to bar crest. Indeed even if alongshore range of cross-shore position of the bar (estimated from the time exposure images) was up to 105 m accounting for an increase of 280 % from the smallest (observed at Transect T 7) to the highest value (observed at Transect T 3), it is not spatially consistent with alongshore variation trend of runup energy.

Interestingly is however the alongshore variations observed in the incident band at the PUV sensor location on the inner bar and the significant regression between the incident band at the PUV and the runup statistics. This suggests that alongshore variability in runup might be driven by wave transformation taking place between the inner bar and the shoreline. Indeed, infragravity motions are generated by nonlinear interactions between high-frequency wind waves (e.g. Herbers et al., 1995, Ruessink, 1998, Hendersen et al., 2006) whose strength might be considerably modulated by wave forcing: the level of wave energy and the shape of the associated energy spectrum (e.g. De Bakker et al., 2015; Norheim et al., 1998) but also the directional spread (e.g. Guza and Feddersen, 2012) and the interaction with surf zone circulation (Howd et al., 1992; Falques ad Iranzo, 1992). Indeed, the presence of the longshore current modifies refraction in the nearshore wave guide and can change the dynamics and kinematics of edge waves (Howd et al., 1992; Falques and iranzo, 1992). Thus currents effects may be accounted in terms of the effective beach profile that play a key role in infragravity energy. De Bakker et al. (2016) using a numerical approach and laboratory data showed that the beach slope affects the nonlinear infragravity-wave interactions and Thomson et al. (2006), analyzing field observations collected near Torrey Pines State Beach in southern California, showed the bottom profile dependence of infragravity waves' energy loss close to the shoreline.

Figure 7 represents synchronized alongshore timestacks generated at different cross location between the shoreline and the inner bar, from the most onshore (left) to the most offshore (right). We clearly observe a huge variability in hydrodyamic patterns including wave dissipation through bathymetric breaking, interactions with the surf zone circulation, wave refraction, harmonic release….

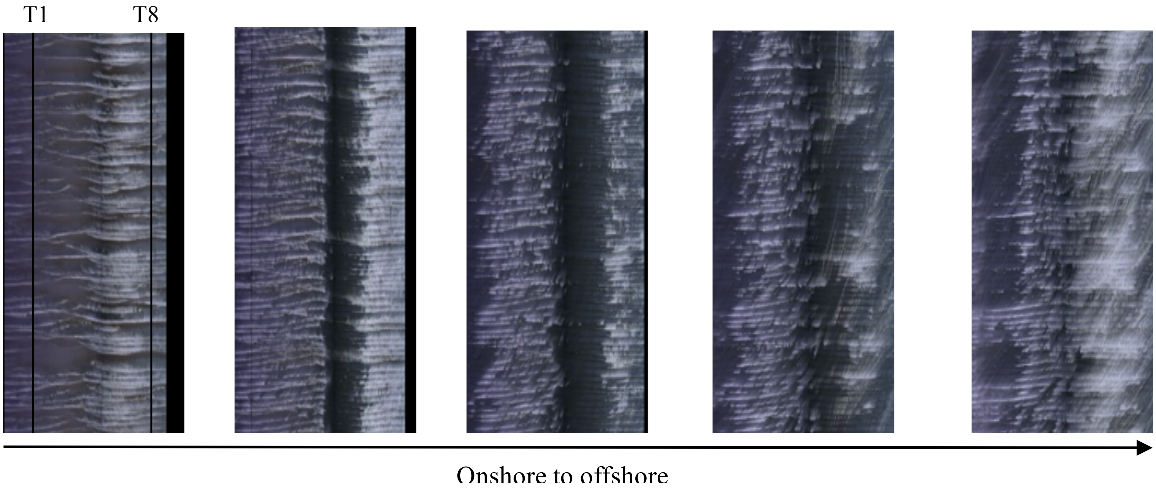

Figure 7. Alongshore synchronized timestacks generated at different cross-shore location between the inner bar and the shoreline illustrating the huge alongshore variability of hydrodynamic processes taking place between the inner bar and the shoreline.

Figure 8, for example shows the estimated bicoherence levels at two transects T 3 and T 8, calculated from the time series of elevations at the PUV sensors. We observe that the bicoherence levels are very low at PUV 3 compared to those observed at PUV 8. In particular the peak of bicoherence between the incident frequency (around 0.075Hz) and the harmonics are not observed at PUV 3. This can be due to the more offshore location of the inner bar crest observed at transect T 3 that will initiate earlier wave breaking than at transect T 8 and thus weaken the strength of the nonlinear couplings, consistent with the results of Sénéchal et al. (2002). However this can also highlight alongshore variability in triad interactions and energy transfer to both higher and lower frequencies. Indeed, at PUV 8, there are also significant peaks in the bicoherence located at frequencies lower than the incident peak, especially in the infragravity band, consistent with observations presented by Ruessink (1998). Detailed image (Figure 9) clearly shows that harmonic release is not uniform alongshore: while energy seems to be transmitted as a multiple crest system with regular wave crest direction at transect T 8, nearly no harmonic decoupling is observed at transect T 1 and wave crest direction are not uniform.

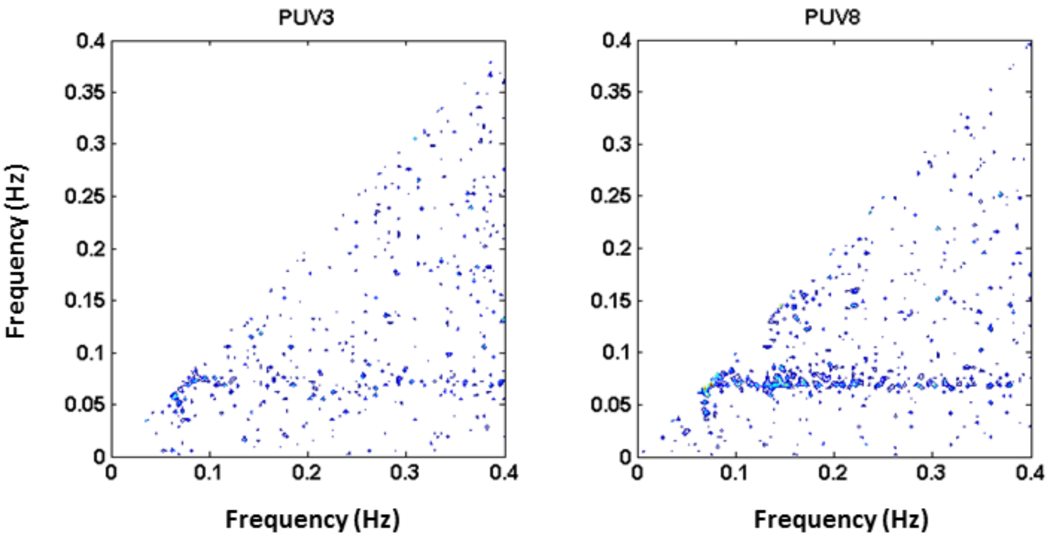

Figure 8. Bicoherence level estimated in the surfzone at two different alongshore positions. Only the contour level significant at 95% are plotted (dof = 84).

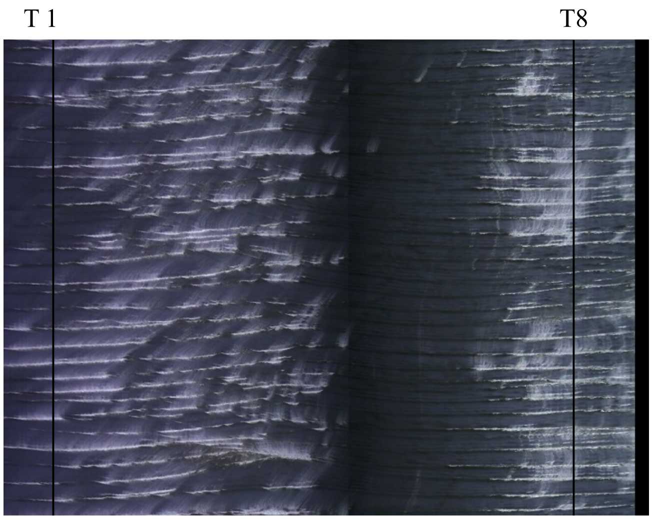

Figure 9. Detailed view of an alongshore timestacks. We clearly observe o the right of the image the released harmonic.

5. Conclusions

Runup time series collected along eight transects in presence of complex beach morphology were observed to present a significant alongshore variability. Runup dynamics was found to be dominant by infragravity energy, consistent with dissipative conditions but presented an alongshore variability of nearly 300%. Analyses of data collected in the surf zone indicated that no such variability is observed. This variability can neither be explained only by alongshore variations in beach slope as observed under similar dissipative conditions nor by variation in the distance from shoreline to bar crest. Data rather suggest that alongshore variability in runup might be driven by wave transformation taking place between the inner bar and the shoreline. In particular, preliminary observations indicate that wave-wave coupling intensity is not uniform along the beach, as well as wave dissipation patterns and wave crest direction. Further analysis are necessary to better quantify the role and the strength of each of these processes.

Acknowledgements
The author would like to thank the DGA and the French navy for providing financial and technical support during the ECORS field experiment and many colleagues (among them Giovanni, Karin, Bob) for the scientific discussions.

References

Almar, R., B. Castelle, B.G. Ruessink, N. Senechal, Bonneton, P., Marieu, V., 2010. Two- and three-dimensional double-sandbar system behaviour under intense wave forcing and a meso-macro tidal range. *Continental Shelf Research*, 30 (7), 781-792.

Bryan, K. R., and G. Coco (2010), Observations of nonlinear runup patterns on plane and rhythmic beach morphology, *J. Geophys. Res.,* 115, C09017, doi:10.1029/2009JC005721.

Butel, R., H. Dupuis, and P. Bonneton, 2002. Spatial variability of wave conditions on the French Aquitanian coast using in-situ data, *In* : *Proceedings 7th International Coastal Symposium (Templepatrick, Northern Ireland), Journal of Coastal. Research*, SI36, 96-108.

Castelle, B., P. Bonneton, H. Dupuis, and N. Sénéchal, 2007. Double bar beach dynamics on the high energy meso-macrotidal French Aquitanian Coast : A review. *Marine. Geology*., 245, 141-159.

Coco, G., Werner, B.T., Burnet, T., and Elgar, S. (2004) The role of tides in beach cusp formation, J. Geophys. Res., 109, CO4011, doi: 10.1029/2003JC002154.

Cohn N., Ruggiero, P., 2016. The influence of seasonal to interannual nearshore profile variability on extreme water levels: modelling wave runup on dissipative beaches. *Coastal Engineering*, 115: 79-92.

De Bakker, A., Herbers, T.H.C., Smit, P.B., Tissier, M.F.S., Ruessink, G. (2015). Nonlinear infragravity-wave interactions on a gently sloping laboratory beach. *Journal of Physical Oceanography*, 45: 589-605.

De Bakker, Tissier, M.F.S., Ruessink, B.G. (2016). Beach steepness effects on nonlinear infragravity-wave interactions: a numerical study. *Journal of Geophysical Research*, 121(1): 554-570.

Falques, A., Iranzo, V. (1992). Edge waves on a longshore shear flow. *Physics of Fluids* 4, 2169, doi: 10.1063/1.858460.

Gallagher, E., J.H.M. MacMahan, Ad Reniers, J. Brown, and Ed Thornton (2011). Grain size variability on a rip-channeled beach. *Marine Geology*, 287(1-4):11.

Guedes, R.M.C., K.R. Bryan, G. Coco, ad R. A. Holman (2012). The effects of tides on swash statistics on an intermediate beach. *Journal of Geophysical Research*, 116, C04008, doi:10.1029/2010JC006660.

Guza, R.T., and E.B., Thornton (1982), Swash oscillations on a natural beach, J. Geophys. Res., 87, 483-491.

Guza, R.T., Feddersen, F. (2012). Effect of wave frequency and directional spread on shoreline runup. *Geophysical Research Letters*. 39(11).

Hendersen, S.M., R.T. Guza, S. Elgar, T.H.C. Herbers, and A.J. Bowen (2006), Nonlinear generation and loss of infragravity wave energy, *J. Geophys. Res*., 111, C12007, doi: 10.129/2006JC003539.

Herbers, T.H.C., S. Elgar, R.T. Guza, and W.C. O'Reilly (1995), Infragravity-frequency (0.005-0.05 Hz) motions on the shelf, II, free waves, *J. Phys. Oceanogr*., 25, 1063-1079.

Holland, K.T. (1995), Foreshore dynamics : swash motions and topographic interactions on natural beaches, Ph.D. thesis, Oreg. State Univ., Corvallis, Oreg.

Holland, K.T., and R.A. Holman (1999), wavenumber-frequency structure of infragravity swash motions, *J. Geophys. Res.*, 104, 13479-13488.

Holman, R.A. (1986), Extreme value statistics for wave run-up on a natural beach, *Coast. Eng*., 9, 527-544.

Holman, R.A., and A.H. Sallenger (1985), setup and swash on a natural beach, *J. Geophys. Res*., 90,945-953.

Howd, P.A., Bowen, A.J., Holman, R.A. (1992). Edge waves in the presence of strong longshore currents. *Journal of Geophysical Research*, 97(C7):11357-11371.

Norheim, C.A., Herbers, T.H.C., Elgar, S. (1998). Nonlinear evolution of surface wave spectra on a beach. Journal of Physical Oceanography, 28: 1534-1551.

Raubenheimer, B., and R.T. Guza (1996), Observations and predictions of run-up, *J. Geophys. Res*., 101, 25575-25587.

Palmsten, M.L., Splinter, K.D. 2016. Observations and simulations of wave runup during a laboratory dune erosion experiment. *Coastal Engineering*, 115:58-66.

Plant, N.G., Stockdon, H.F. 2015. How well can wave runup be predicted? Comment on Laudier et al. (2011) and Stockdon et al. (2006). *Coastal Engineering*, 102:44-48.

Peregrine, D.H., Williams, S.M., 2001. Swash overtopping a truncated plane beach. *J. Fluid Mech*. 440: 391-399.

Raubenheimer, B., R.T. Guza, S., Elgar, and N. Kobayashi (1995), Swash on a gently sloping beach, *J. Geophys. Res.*, 100, 8751-8760.

Ruessink, B.G. (1998). The temporal and spatial variability of infragravity energy in a barred nearshore zone. *Continental Shelf Research*, 18, 585-605.

Ruessink, B.G., M.G., Kleinhans, and P.G.L., Van den Beukel (1998), Observations of swash under hihly dissipative conditions, *J. Geophys. Res*., 103, 3111-3118.

Ruggiero, P., P.D., Komar, J.J., Marra, W.G. McDougal, and R.A. Beach (2001), Wave runup, extreme water levels and the erosion of properties backing beaches, *J. Coastal Res*., 17, 407-419.

Ruggiero, P., R.A., Holman, and R.A. Beach (2004), Wave run-up on a high-energy dissipative beach, *J. Geophys. Res*, 109, C06025, doi:10.1029/2003JC002160.

Sallenger, A.H., 2000. Storm impact scale for barrier islands. *Journal Of coastal Research*, 16 (3): 890-895.

Senechal, N., Bonneton, P., Dupuis, H. (2002). Field experiment on secondary wave generation on a barred beach ad the consequent evolution of energy dissipation on the beach face. *Coastal Engineering*, 46: 233-131.

Senechal, N., Gouriou, T., Castelle, B., Parisot, J.-P., Capo, S., Bujan, S., Howa, H. (2009). Morphodynamic response of a maso- to macro-tidal intermediate beach based on a long-term data set, *Geomorphology*, 107:263-274.

Senechal, N., S. Abadie, F. Ardhuin, E. Gallagher, J.H.M. MacMahan, G. Masselink, H. Michallet, Ad J.H.M. Reniers, B.G. Ruessink, P.E. Russell, D. Sous, I.L. Turner, P. Bonneton, S. Bujan, S. Capo, R. Certain, T. Garlan, R. Pedreros (2011a), The ECORS-Truc Vert'08 field beach experiment: Presentation of a three-dimensional morphologic system in a macro-tidal environment during consecutive extreme storm conditions. *Ocean Dynamics*. doi: 10.1007/s10236-011-0472-x.

Senechal, N., G. Coco, K.R. Bryan, ad R.A. Holman (2011b). Wave runup during extreme storm conditions. *Journal of Geophysical Research*, 116, C07032, doi:10.1029/2010JC006819.

Senechal, N., ., Coco, G., Bryan, K., MacMahan, J., Brown, J., Holman, R. (2013). Tidal effects I presence of complex 3D morphologies under dissipative surf zone conditions. *In proceeding of Coastal Dynamics 2013* – Arcachon – France.

Stockdon, H.F., R.A. Holman, P.A. Howd, and A.H., Sallenger Jr. (2006), Empirical parameterization of setup, swash and runup, Coast. Eng., 53, 573-588.

Thomson, J., S. Elgar, B. Raubenheimer, T.H.C. Herbers, and R.T. Guza (2006), Tidal modulation of infragravity waves via nonlinear energy losses in the surf zone, *Geophys. Res. Lett*., 33, L05601, doi: 10.1029/2005GL025514.

Wright, L.D., A.D. Short, and M.O. Green, 1984. Morphodynamic variability of surf zones and beaches: A synthesis. *Marine Geology*, 56, 93-118.